Industrial Crops and Products 73 (2015) 28–40

Contents lists available at ScienceDirect

Industrial Crops and Products

journal homepage: www.elsevier.com/locate/indcrop

Phenolic screening by HPLC–DAD–ESI/MS^n and antioxidant capacity of leaves, flowers and berries of *Rubus grandifolius* Lowe

Sandra C. Gouveia-Figueira[a,b,*], Paula C. Castilho[b]

[a] Department of Chemistry, Umeå University, Sweden
[b] Centro de Química da Madeira, CCCEE, Universidade da Madeira Campus Universitário da Penteada, Piso 0, 9000-390 Funchal, Portugal

ARTICLE INFO

Article history:
Received 15 November 2014
Received in revised form 7 March 2015
Accepted 9 March 2015
Available online 29 April 2015

Keywords:
Rubus
Berries
Phenolic compounds
HPLC–DAD–ESI/MS^n
Antioxidant

ABSTRACT

In Madeira Island (Macaronesia Island), *Rubus grandifolius* Lowe berries, locally known by *amoras*, are widely consumed fresh or processed as jam, juice or liquor. Folk medicine describes *R. grandifolius* Lowe fruits and leaves being used to treat diabetes, as depurative, diuretic and to relieve sore throat.

The aim of this study was to investigate phenolic composition and antioxidant capacity of the different edible parts of the plant (berries, leaves and flowers). HPLC–DAD–ESI/MS^n was used to establish the phenolic profile. Phenolic monomers such as flavonol *O*-glycosilated (quercetin and kaempferol), quinic acid and caffeic acid conjugates were characterized using the electrospray source in the negative mode; while positive mode was employed to detect glycosylated anthocyanins (cyanidin, delphinin and petunidin).

The berries presented a higher radical scavenger capacity (DPPH and ABTS assays) and reducing properties (FRAP) than the leaves and the flowers. Ethanolic extracts showed highest antioxidant capacity when compared with water based extracts: DPPH values of 147.9 ± 0.7 μmol eq Trolox/g DM; ABTS value of 255.8 ± 1.9 μmol eq Trolox/g DM and FRAP value 9455 ± 29 mmol Fe(II)/mgDM).

1. Introduction

Plants of the genus *Rubus* (more than 740 species) are well known, mainly due to the use of their fruits in food industry, such as raspberry, blackberry or redberry. They are consumed either as fresh fruits or processed food (Bobinaitė et al., 2012) and associated to a wide range of biological activities such as antioxidant, antimicrobial, anti-carcinogenic (Bobinaitė et al., 2012), reduces the risk of cardiovascular accidents and neurodegenerative diseases (Kusznierewicz et al., 2012), etc. They are source of nutrients (vitamin A and C), fatty acids, fiber and secondary metabolites, mainly phenolic compounds (Jaakkola et al., 2012).

Three main classes of phenolic compounds were identified in *Rubus* fruits, anthocyanins, ellagitannins and phenolic monomers. Phenolic monomers include phenolic acids (hydroxycinnamic and hydroxybenzoic acids) and flavonoids either free and/or as glycosylated aglycones (catechin, epicathechin, quercetin and kaempferol). Their occurrence, type and amount can vary remarkably given different factors for example genetic, environmental and/or processing, harvesting, storage and analysis (Bobinaitė et al., 2012).

The separation and detection of phenolic compounds in complexes matrixes such as plant/fruits extracts has been performed with different techniques. Reversed-phase high-performance liquid chromatography (RP-HPLC) coupled with UV diode-array detector (DAD) and tandem mass spectrometry detector (MS/MS) with electrospray (ESI) or atmospheric pressure chemical ionization (APCI) has proved to be the most suitable for the unambiguous structural identification and quantification of phenolic compounds (Scordino and Sabatino, 2014).

The use of ESI in negative mode is clearly more sensitive and selective for analyzing phenolic compounds (Gouveia and Castilho, 2010). With tandem mass spectrometry (MS^n), it is possible to get a large set of structural data which is not possible with UV data.

The aerial parts of *Rubus* genus have been studied in a less extent than the berries and recently Hummer (Hummer, 2010) published a detailed review about their pharmacological activity in ancient medicine and also in folk medicine in different parts of the world.

Rubus grandifolius Lowe is a rare plant endemic to Madeira Archipelago (Portugal) which inhabits in moist and shady areas. It has hardy and arcuate stems with prickles, ovate-oblong leaves and numerous white flowers borne in a large pyramidal panicle. The berries are fleshy, subspherical to cylindrical fruit that becomes black when mature. (Turland, 1994) The berries are used mainly in food industry, as jam, juice and liquor.

* Corresponding author. Present address: Kemihuset, Linnaeus väg 10, KB6A14 Umeå Universitet, SE-901 87 Umeå Sverige. Tel.: +46 907865182.
E-mail address: sandra.gouveia@chem.umu.se (S.C. Gouveia-Figueira).

http://dx.doi.org/10.1016/j.indcrop.2015.03.022
0926-6690/

The leaves, shoots and fruits are described in the folk medicine as astringent for children and also as remedy for diabetes, depurative, diuretic and to relieve sore throat (Rivera and Obón, 1995) and are prepared as herbal teas or alcoholic infusions. The goal of this work was to characterize the phenolic composition of the extracts of the leaves, flowers and fruits of *R. grandifolius* Lowe by HPLC–DAD–ESI/MS^n.

2. Material and methods

2.1. General experimental procedures

The HPLC separation was done using a Dionex ultimate 3000 series instrument (California, EUA) equipped with a binary pump, a diode-array detector (DAD), an autosampler and a column compartment with temperature control.

Tandem mass spectrometry was performed with a model 6000 ion trap mass spectrometer (Bruker Esquire, Bremen, Germany) fitted with an ESI source. Esquire control software was used to data acquisition and processing.

The following chemicals were purchased from Chengdo Biopurify Phytochemicals, Ltd., China (Sichuan, China). 1,3-*O*-Dicaffeoylquinic acid, 1,5-*O*-dicaffeoylquinic acid, 3,4-*O*-dicaffeoylquinic acid, 3,5-*O*-dicaffeoylquinic acid, 4,5-*O*-dicaffeoylquinic acid and 3,4,5-*O*-tricaffeoylquinic acid (>98% by HPLC for all). The following reagents were obtained from Merck (Darmstadt, Germany): potassium persulfate (99%), sodium chloride (99.5%), disodium phosphate dodecahydrated (99%), glacial acetic acid (100%), sodium carbonate (p.a.) and ferrous sulfate heptahydrate (99%). 2,2-Diphenyl-1-picrylhydrazyl (DPPH) (>95%), Trolox (≥99.8%, HPLC), 2,2′azinobis-(3-ethylbenzthiazoline-6-sulfonic acid) (ABTS) (≥99%, HPLC) and 2,4,6-tri(2-pyridyl)-*s*-triazine (TPTZ) (≥99.0%, TLC) were purchased from Fluka (Lisbon, Portugal). Potassium chloride (>99.5%), gallic acid (99%, HPLC) and potassium acetate (p.a.) were purchased from Panreac (Barcelona, Spain).

All solvents used for plant solid–liquid extraction were AR grade, purchased from Fisher (Lisbon, Portugal). HPLC–MS grade acetonitrile (99.9%, LabScan, Gliwice, Poland) and ultra-pure water (Milli-Q water purification system, EUA) were used for HPLC analysis.

Standards stock solutions were prepared in ethanol (100 μg/mL): quercetin (>99%), *p*-coumaric acid (>99%) and caffeic acid (>99%) from Extrasynthese (Lyon, France), kaempferol (>99%) and 5-*O*-caffeoylquinic acid (99%) from Acros Organics (Geel, Belgium).

2.2. Plant material collection and sample preparation

Samples of *R. grandifolius* were collected in the wild in Santo da Serra, Madeira Island. The plant material comprised individually separated leaves, flowers and berries (amoras). Flowers and leaves were collected during the month of May and fruits in July. The plants were authenticated by taxonomist Fátima Rocha and vouchers of leaves and flowers were deposited in the Madeira Botanical Garden herbarium collection.

The leaves and flowers were dried in the dark and at room temperature (20 °C) for one week; ground to fine powder in a mechanic grinder to 60 mesh size (Sejali and Anuar, 2011) and submitted to ultrasound-assisted solvent extraction: 1 g of plant material was extracted with 25 mL methanol using a sonicator Bandelin Sonorex (Germany) at 35 kHz and 200 W for 60 min at 20 °C.

Samples of fresh, ripe wild berries were hand harvested and frozen at −20 °C. Before analysis, they were ground and extracted as described for the leaves and flowers. The extraction solvents were 100% ethanol and 100% water and ultrasound-assisted extraction was done in the same conditions as described above.

Filtered extracted solutions were concentrated using a rotary evaporator (40 °C). Each dried extract was dissolved in initial HPLC mobile phase (CH_3CN/H_2O (20/80, v/v)) at a concentrations (m/v) of 5 mg/mL and filtered through 0.45 mm Nylon micropore membranes. Ten microliter were injected for HPLC–DAD–ESI/MS^n analysis and for each sample three independent extractions were performed.

2.3. HPLC–DAD–ESI/MS^n analysis

2.3.1. Liquid chromatography

Samples were separated using a Phenomenex Gemini C_{18} column (5 μm, 250 × 3.0 mm i.d.; Phenomenex) at 30 °C. Acetonitrile (A) and water/formic acid (100/0.1, v/v) (B) were used as eluents and the following gradient was used: 20% A (0 min), 25% A (10 min), 25% A (20 min), 50% A (40 min), 100% A (42–47 min), 20% A (49–55 min). The flow rate was set at 0.4 mL/min; the DAD chromatograms were recorded at 280 nm and 350 nm and spectral data for all peaks were accumulated in the range of 190–400 nm.

2.3.2. Mass spectrometry

Negative and positive ionization mode was used in the range *m*/*z* 100–1000 at a scan speed of 13,000 Da/s. High purity nitrogen (N_2) was used both as drying gas (10.0 mL/min) and as a nebulizing gas at a pressure of 50 psi. The nebulizer temperature was set at 365 °C and capillary voltage was +400 V. Helium (He, Ultra-high-purity) was used as collision gas at a pressure of 1×10^{-5} mbar and the collision energy was fixed at 40 V. MS^n data were acquired in auto MS^n mode(isolation width of 4.0 *m*/*z*). For MS^n analysis, the mass spectrometer scanned from 10 to 1000 *m*/*z* with fragmentation amplitude of 1.0 V (MS^n up to MS^4) and two precursor ions.

2.4. DPPH radical scavenging activity

Sample solutions (100 μL, 10 mg/mL) were added to 3.5 mL methanol DPPH radical solution (0.06 mM) (Gouveia and Castilho, 2012b). The decrease in absorbance (λ = 516 nm) was measured during 30 min. The DPPH radical scavenging effect was expressed as μmol Trolox eq per 100 g of dried plant (μmol eq Trolox/100 g dried plant).

2.5. $ABTS^{\bullet+}$ radical scavenging activity

The ABTS assay initially reported by Re et al. (1999) was used with some modifications. Briefly, the $ABTS^{\bullet+}$ radical was prepared by mixing 50 mL of $ABTS^{\bullet+}$ solution (2 mM) with 200 μL of $K_2S_2O_8$ solution (70 mM). This mixture was stored in the dark for 16 h, at room temperature. On a daily basis the $ABTS^{\bullet+}$ solution was diluted with pH 7.4 phosphate buffered saline (PBS) solution to an initial absorbance of 0.700 ± 0.019 at 734 nm. For the assessment of the radical scavenging activity, an aliquot of 100 μL methanolic solution with a concentration (w/v) of 10 mg/mL was added to 1.8 mL of $ABTS^{\bullet+}$ solution and the absorbance decrease (λ = 734 nm) was recorded during 6 min. Results were expressed in terms of μmol Trolox eq per 100 g of dried plant antioxidant capacity (μmol eq Trolox/100 g Trolox/100 g dried plant).

2.6. Ferric reducing activity (FRAP assay)

FRAP reagent was prepared by mixing 2.5 mL of solution $FeCl_3 \cdot 6H_2O$ (20 mM), 2.5 mL of solution TPTZ (10 mM in 40 mM of HCl) and 25 mL of acetate buffer 0.3 M (pH 3.6) and incubating at 37 °C. Thirty microliter of extract methanolic solution

(1 mg/mL) were added to 180 μL of distilled water and 1.8 mL of FRAP solution (prepared fresh). The increase of absorbance was recorded (λ = 593 nm) during 30 min at 37 °C. The FRAP results were expressed as mmol $FeSO_4 \cdot 7H_2O$ per mg of dried plant (mmol Fe(II)/mg) (Gouveia and Castilho, 2012a).

3. Results and discussion

3.1. HPLC–DAD–ESI/MS^n analysis

Ultrasound extraction was selected to recover the phenolic compounds of *R. grandifolius* Lowe (flowers, leaves and berries). More than 40 compounds were detected and typical hydroxycinnamic acid derivatives UV absorptions (λ_{max} 230–240, 300sh. 320–340 nm) and anthocyanins (λ_{max} 510–530 nm) were observed (Mabry et al., 1970).

Two components were undoubtedly identified by comparing (HPLC retention time, UV and mass spectra) with commercially standard compounds. MS^n fragmentation mechanisms combined with UV data were used to propose the structures of the remaining peaks. However, several minor peaks remained unidentified.

Tables 1 and 2 show the analytical parameters determined: retention time (t_R), wavelength of maximum absorbance (λ_{max}), deprotonated molecular ions $[M-H]^-$ and $[M+H]^+$, respectively, and major diagnostic fragment ions of the most intense peaks, in negative and positive mode, respectively. Chemical structures of compounds detected in negative and positive mode are show in Figs. 1 and 2, respectively. The base peak chromatogram (BPC) obtained for the phenolic profile is presented in Fig. 3 and BPC for anthocyanins separation in Fig. 4.

3.1.1. Negative mode ionization

Compound **1** (t_R = 2.7 min) displayed a $[M-H]^-$ ion at *m/z* 683. MS^2 fragmentation of the ion at *m/z* 683 gave a fragment ion at *m/z* 341 suggesting a dimmer. Further fragmentation gave a fragment ion at *m/z* 179 [caffeic acid – H]$^-$. Therefore, based on these data and according to literature (Gouveia and Castilho, 2010), compound **1** was assigned as a dimmer of caffeic acid *O*-hexoside.

Compound **2** (t_R = 3.3 min) gave a $[M-H]^-$ ion at *m/z* 191 and its MS^2 fragmentation resulted in a fragment base peak ion at *m/z* 127 suggesting a quinic acid. This compound was found in all samples.

Compound **3** (t_R = 4.0 min) exhibited a $[M-H]^-$ ion at *m/z* 341, and its fragmentation showed fragment ion at *m/z* 179. This compound corresponds to a caffeic acid-*O*-hexoside only present in the leaves.

Compound **4** (t_R = 4.2 min) and **6** (t_R = 5.0 min) gave $[M-H]^-$ ions at *m/z* 353. For compound **4**, the MS^2 fragmentation gave a fragment ion at *m/z* 191, as base peak, and an intense ion at *m/z* 179 (65.5% of base peak). Based on the hierarchical key proposed by Clifford et al. (2005) and our recent work (Gouveia and Castilho, 2010) this compound was identified as 3-*O*-caffeoylquinic. Compound **6** was identified as 5-*O*-caffeoylquinic acid based on comparison with a standard compound.

Compounds **5** (t_R = 4.8 min) and **12** (t_R = 7.6 min) gave a $[M-H]^-$ ion at *m/z* 577 and were characterized as procyanidin dimers. The MS^4 fragmentation gave fragment ions at *m/z* 289, as base peak. This fragment corresponds to a monomer catechin and this loss is related to the cleavage of the interflavanoid C–C linkage (Soong and Barlow, 2005). The MS^2 fragment ions, such as the base peak at *m/z* 425 (loss of 152 Da), are formed from a RDA reactions and it eliminates a water molecule (−18 Da) to form a fragment ion at *m/z* 407. This fragmentation pattern is consistent with procyanidin dimers of the type(epi) catechin-(epi) catechin (Kajdžanoska et al., 2010) also named procyanidin B2. (Soong and Barlow, 2005)

Compound **7** (t_R = 5.4 min) showed a $[M-H]^-$ at *m/z* 355 and in the MS^2 fragmentation an ion at *m/z* 161 was observed. This fragment ion is formed due to the loss of 194 Da, possibly a ferulic acid unit. The ion at *m/z* 161 ([hexose–H_2O–H]$^-$) gave a MS^3 ion at *m/z* 133 indicating a malic acid residue (Tang et al., 2011). Thus, compound **7** was characterized as a ferulicmalic acid derivative.

Compound **10** (t_R = 6.2 min) gave a $[M-H]^-$ at *m/z* 493 (Fig. 5). The MS^2 fragmentation gave a fragment ion at *m/z* 179 (base peak), and an intense fragment ion at *m/z* 341 (loss of 152 Da; 83.3% of base peak). Further fragmentation of this ion indicates a caffeic acid *O*-hexoside moiety (comparison with compound **3**). The 152 Da residue was identified as a galloyl unit linked to the hexoside group (Kajdžanoska et al., 2010). Thus, compound **10** was characterized as caffeic acid -*O*-galloylhexoside.

Compound **11** (t_R = 7.0 min) showed a $[M-H]^-$ at *m/z* 609. Its MS^2 fragmentation gave a fragment ion at *m/z* 301 due to a neutral loss of 308 Da (probably two sugar units 162 + 146 Da). Since the aglycone radical ion was not found in the MS^2 spectrum and given the rules described by Ablajan et al. (2006), this compound was characterized as being a flavonoid mono-*O*-diglycoside. The MS^2 spectrum did not show fragment ions attributed to the glycan part, Y_n^- and gave a base peak correspondent to the deprotonated aglycone ion, Y_0^-. This behavior is typical for diglycosides with (1 → 6) interglycosidic linkage (*O*-rutinoiside residue) (Cuyckens and Claeys, 2004). It was not possible to establish the exact glycosilation position but positions 7-OH and 3-OH were excluded by comparison with a reference standard and compound **11** was characterized as quercetin-*O*-rutinoside.

Compound **14** (t_R = 8.4 min) yielded a $[M-H]^-$ ion at *m/z* 463 and its MS^2 fragmentation gave the aglycone fragment ion (Y_0^-) at *m/z* 301 (−162 Da, probably an hexoside residue). The MS^n fragmentation gave fragment ions from retro-Diels–Alder reaction at *m/z* 151 ($^{1,2}A^-$ – CO), 179 ($[^{1,2}A^- - H]^-$), 255 ([M–H–H_2O–CO]$^-$) and 271 ([M–H–CH_2O]$^-$) (Cuyckens and Claeys, 2004). These MS^n data matches the fragmentation of a standard quercetin solution (data not showed) and consequently quercetin should be the aglycone of compound **14**.

It is known that, despite that all the hydroxyl are available, 3-OH and 7-OH positions are regular glycosylation sites for flavonols (Cuyckens and Claeys, 2005).

Glycosilation at position 3-OH for compound **14** was excluded by comparison of its MS^n fragments and UV data (bands at λ = 258 nm and 353 nm) to those obtained for a standard solution of quercetin-3-*O*-glucoside. Thus, compound **14** was tentatively identified as quercetin-7-*O*-hexoside.

Compound **15** (t_R = 8.7 min) displayed a $[M-H]^-$ ion at *m/z* 607 and further MS^n fragmentation lead to typical fragments of a quercetin-7-*O*-hexoside as described for compound **14** (Fig. 6). The MS^2 spectrum showed three main fragments at *m/z* 545 (loss of 62 Da), *m/z* 505 (loss of 102 Da) and *m/z* 463 (loss of 144 Da). This fragmentation pattern has been previous described for other flavonoid glycosides (Pereira et al., 2012) as 3-hydroxy-3-methylglutaroyl. The exact position of this moiety is hard to define. Therefore, compound **15** was characterized as a 3-hydroxy-3-methylglutaroyl of quercetin-7-*O*-hexoside (Fig. 7).

Compound **17** (t_R = 9.2 min) showed a $[M-H]^-$ ion at *m/z* 593 and in the MS^2 fragmentation lost a neutral fragment of 308 Da, yielding a fragment ion at *m/z* 285. This ion displayed typical RDA fragment of kaempferol (Y_0–H–CO, *m/z* 257; Y_0–2CO, *m/z* 229 and $^{1,3}A^-$, *m/z* 151). The moiety of 308 Da, can possibly be composed of a coumaroyl or rhamnose (146 Da) and caffeoyl or hexoside groups (162 Da).

Compound **18** (t_R = 10.1 min) presented a $[M-H]^-$ ion at *m/z* 477. MS^n fragmentation this ion showed the elimination of a glucuronic acid residue (loss of 176 Da) and the deprotonated aglycone ion at *m/z* 301. The MS^3 spectrum of the aglycone ion gave

Table 1
Characterization of phenolic compounds of the extracts of leaves, flowers and berries (amoras) from *Rubus grandifolius* Lowe by HPLC–DAD/ESI–MS^n in negative mode.

No.	t_R (min)	UV λ_{max} (nm)	$[M-H]^-$ m/z	HPLC–DAD–ESI/MS^n *m/z* (% base peak)	Assigned identity	Sample
1	2.7	224, 300	683	MS^2 [683]: 341 (100) MS^3 [683 → 341]: 251 (11.3), 179 (51.5), 161 (100)	Dimmer caffeic acid-*O*-hexoside	Leaves Flowers Amoras ethanol Amoras water
2	3.3	–	191	MS^2 [191]: 173 (100), 127 (39.1), 111 (36.7), 93 (29.9) MS^3 [191 → 173]: 111 (100)	Quinic acid	Leaves Flowers Amoras ethanol Amoras water
3	4.0	–	341	MS^2 [341]: 281 (100), 251 (71.3), 179 (56.3) MS^3 [341 → 281]: 221 (21.8), 179 (100), 135 (18.1) MS^4 [341 → 281 → 179]: 136 (14.2), 135 (100)	Caffeic acid-*O*-hexoside	Leaves
4	4.2	242, 300, 325	353	MS^2 [353]: 191 (100), 179 (65.5), 135 (13.5) MS^3 [353 → 191]: 173 (36.5), 171 (66.2), 127 (100) MS^4 [353 → 191 → 127]: 109 (100), 99 (91.8)	3-*O*-Caffeoylquinic acid	Leaves Flowers
5	4.8	–	577	MS^2 [577]: 451 (23.7), 425 (100), 407 (69.6), 289 (29.0) MS^3 [577 → 425]: 408 (17.7), 407 (100) MS^4 [577 → 425 → 407]: 289 (100), 281 (85.7), 256 (53.1), 213 (38.6), 199 (30.4)	Procyanidin B2	Leaves
6[a]	5.0	242, 300, 325	353	MS^2 [353]: 191 (100) MS^3 [353 → 191]: 173 (59.7), 171 (100), 111 (59.1)	5-*O*-Caffeoylquinic acid	Flowers
7	5.4	–	355	MS^2 [355]: 161 (100) MS^3 [355 → 161]: 133 (100)	Ferulicmalic acid derivative	Leaves Flowers
8	5.7	–	675	MS^2 [675]: 640 (26.9), 639 (100) MS^3 [675 → 639]: 459 (88.9), 315 (89.7), 314 (100), 300 (92.2), 299 (51.7) MS^4 [675 → 639 → 314]: 301 (10.2), 300 (77.0), 299 (100)	Unknown	Flowers
9	6.0	–	595	MS^2 [595]: 445 (29.1), 301 (70.4), 300 (100), 271 (21.2) MS^3 [595 → 300]: 273 (21.0), 271 (62.5), 255 (100), 179 (37.3)	Unknown	Flowers
10	6.2	300	493 (100)	MS^2 [493]: 341 (83.3), 251 (92.6), 221 (45.4), 179 (100) MS^3 [493 → 251]: 179 (100), 135 (11.7) MS^4 [493 → 251→]: 135 (100)	Caffeic acid-*O*-galloylhexoside	Leaves
11	7.0	257, 353	609	MS^2 [609]: 590 (14.1), 300 (33.7), 301 (100) MS^3 [609 → 301]: 194 (16.3), 179 (18.0), 163 (15.8), 151 (100)	Quercetin-*O*-rutinoside	Leaves Flowers Amora ethanol

Table 1 (*Continued*)

No.	t_R (min)	UV λ_{max} (nm)	$[M-H]^-$ m/z	HPLC–DAD–ESI/MS^n *m/z* (% base peak)	Assigned identity	Sample
12	7.6	–	577	MS^2 [577]: 451 (21.9), 425 (100), 407 (61.2) MS^3 [577 → 425]: 407 (100), 187 (18.8), 137 (60.5) MS^4 [577 → 425 → 407]: 389 (27.9), 255 (34.7), 289 (100)	Procyanidin B2	Leaves
13	8.1	–	509	MS^2 [509]: 491 (100), 473 (37.3), 461 (39.7), 367 (74.7), 163 (2.4) MS^3 [509 → 491]: 473 (33.0), 461 (100), 179 (13.6)	Unknown	Leaves Flowers
14	8.4	285, 352	463	MS^2 [463]: 302 (20.0), 301 (100), 300 (41.0) MS^3 [463 → 301]: 271 (30.5), 179 (100), 151 (66.9) MS^4 [463 → 301 → 179]: 169 (14.7), 151 (100)	Quercetin-7-*O*-hexoside	Flowers Amora ethanol
15	8.7	260, 352	607	MS2 [607]: 545 (4.5), 505 (13.6), 464 (22.), 463 (100) MS3 [607 → 463]: 301 (100), 300 (42.3), 151 (33.6) MS4 [607 → 463 → 301]: 271 (86.3), 255 (84.0), 254 (95.1), 179 (86.3), 151 (100), 121 (79.8)	3-Hydroxy-3-methylglutaroyl of quercetin-7-*O*-hexoside	Amora ethanol Amoras water
16	8.9	–	523	MS^2 [523]: 476 (23.0), 475 (100) MS^3 [523 → 475]: 432 (32.4), 329 (100), 327 (47.2), 301 (24.0) MS^4 [523 → 475 → 329]: 314 (100), 283 (40.0)	Unknown	Leaves Flowers
17	9.2	–	593	MS^2 [593]: 285 (100) MS^3 [593 → 285]: 257 (100), 229 (69.0), 151 (28.7), MS^4 [523 → 475 → 329]: 314 (100), 283 (40.0)	Kaempferol derivative	Flowers
1819	10.1	–	477 (100) 433 (58.8)	MS^2 [477]: 302 (21.9), 301 (100) MS^3 [477 → 301]: 257 (13.9), 179 (83.9), 151 (100) MS^4 [477 → 301 → 151]: 107 (100) MS^2 [433]: 301 (100), 300 (86.5) MS^3 [433 → 301]: 283 (5.3), 271 (100), 255 (63.8), 179 (36.2), 151 (62.5) MS^4 [433 → 301 → 271]: 229 (62.2), 201 (100)	Quercetin-*O*-glucuronide Ellagic acid-*O*-pentoside	Leaves Flowers
20	10.8	271, 355	477	MS^2 [477]: 327 (10.1), 285 (100), 284 (59.5), 255 (21.6) MS^3 [477 → 285]: 257 (58.0), 255 (100), 229 (22.6), 227 (29.8) MS^4 [477 → 285 → 255]: 255 (100), 229 (43.0), 185 (23.2)	Kaempferol-*O*-hydroxylferuloyl	Leaves
21	11.0	–	447	MS^2 [447]: 299 (25.5), 285 (70.3), 284 (100) MS^3 [447 → 285]: 257 (100), 229 (78.0), 151 (47.4)	Kaempferol-3-*O*-hexoside	Flowers
22	11.7	–	337	MS2 [337]: 293 (34.8), 279 (17.0), 191 (100), 147 (19.0) MS3 [337 → 191]: 147 (100) MS4 [337 → 191 → 147]: 103 (100)	1-*O*-*p*-coumaroylquinic acid	Amoras ethanol
23	11.8	–	503	MS^2 [503]: 341 (86.8), 281 (53.8), 251 (91.3), 221 (49.0), 179 (100) MS^3 [503 → 179]: 136 (14.0), 135 (100)	Caffeic acid-*O*-dihexoside	Leaves
24	12.3	271, 355	461	MS^2 [461]: 286 (16.8), 285 (100) MS^3 [461 → 285]: 257 (100), 229 (68.4), 197 (76.5), 173 (59.2), 163 (77.0) MS^4 [461 → 285 → 257]: 239 (100), 229 (29.6), 163 (54.9)	Kaempferol-7-*O*-glucuronide	Leaves Flowers
25	12.4	271, 356	417	MS^2 [417]: 285 (35.1), 284 (100), 283 (11.5) MS^3 [417 → 284]: 257 (35.2), 255 (100), 241 (35.2)	Kaempferol-3-*O*-pentoside	Flowers
26[a]	12.5	242, 300, 327	515	MS^2 [515]: 354 (12.8), 353 (100) MS^3 [515 → 353]: 191 (100)	1,5-*O*-dicaffeoylquinic	Flowers
27	12.9	–	487	MS^2 [487]: 444 (18.7), 323 (100), 221 (35.0), 161 (57.2) MS^3 [487 → 323]: 263 (37.8), 221 (100), 179 (39.2), 135 (38.2) MS^4 [487 → 323 → 221]: 177 (100)	Unknown	Leaves

28	13.1	–	489	MS^2 [489]: 446 (86.3), 445 (100), 442 (69.1), 402 (72.6) MS^3 [489 → 445]: 401 (100), 359 (21.4), 357 (16.8) MS^4 [489 → 445 → 401]: 357 (100)	Unknown	Amora ethanol
29	13.6	–	547	MS^2 [547]: 323 (23.7), 281 (23.0), 179 (45.0), 161 (100) MS^3 [547 → 161]: 133 (100)	Umbelliferone	Leaves
30	14.3	–	695	MS^2 [695]: 533 (24.3), 486 (32.6), 485 (100) MS^3 [695 → 485]: 468 (27.2), 467 (100), 441 (18.3) MS^4 [695 → 485 → 467]: 424 (34.5), 423 (100), 379 (10.5)	Unknown	Flowers
31	15.0	–	711	MS^2 [711]: 665 (12.3), 504 (41.4), 503 (100) MS^3 [711 → 503]: 486 (23.3), 485 (100), 453 (17.6), 409 (11.3) MS^4 [711 → 503 → 485]: 453 (100), 423 (90.1), 409 (52.3), 403 (77.9), 401 (86.5)	Triterpen acid-*O*-hexoside acetyl	Leaves Flowers Amoras ethanol
32	15.7	–	679	MS^2 [679]: 518 (31.4), 517 (100), 499 (24.8), 437 (13.7) MS^3 [679 → 517]: 499 (100), 471 (18.2), 455 (21.2), 437 (41.5) MS^4 [679 → 517 → 499]: 481 (24.9), 455 (79.8), 437 (100)	Ganoderic acid hexoside	Leaves Flowers Amoras ethanol
33	18.3	–	711	MS^2 [711]: 665 (18.1), 504 (20.3), 503 (100) MS^3 [711 → 503]: 485 (100), 485 (100), 459 (48.0), 442 (44.6), 409 (11.3) MS^4 [711 → 503 → 485]: 441 (100), 421 (26.8), 401 (24.7)	Triterpen acid-*O*-hexoside acetyl	Flowers Amoras ethanol
34	19.0	–	479	MS^2 [479]: 385 (100) MS^3 [479 → 385]: 291 (100), 196 (27.6) MS^4 [479 → 385 → 291]: 197 (100)	Unknown	Leaves
35	22.7	–	709	MS^2 [709]: 502 (26.2), 501 (100) MS^3 [709 → 501]: 422 (81.2), 421 (100), 403 (90.4), 369 (57.4) MS^4 [709 → 501 → 421]: 403 (100), 395 (48.4), 387 (50.6), 369 (52.9)	Unknown	Leaves Flowers Amoras ethanol
36	24.2	–	709	MS^2 [709]: 663 (16.1), 502 (30.7), 501 (100) MS^3 [709 → 501]: 484 (12.8), 483 (100), 367 (10.7) MS^4 [709 → 501 → 483]: 439 (50.9), 438 (100)	Unknown	Leaves Flowers Amoras ethanol
37	24.8	–	711	MS^2 [711]: 504 (34.0), 503 (100) MS^3 [711 → 503]: 485 (32.6), 442 (33.3), 441 (100), 421 (16.2) MS^4 [711 → 503 → 441]: 423 (93.7), 401 (76.3), 171 (100)	Triterpen acid-*O*-hexoside acetyl	Leaves
38	25.6	–	593	MS^2 [593]: 447 (12.2), 286 (11.0), 285 (100) MS^3 [593 → 285]: 257 (100), 256 (80.9), 229 (61.0), 199 (34.8), 151 (70.3) MS^4 [593 → 285 → 257]: 230 (100), 212 (88.6)	Kaempferol-*O*-coumaroyl hexoside	Leaves Flowers
39	25.9	–	679	MS^2 [679]: 559 (15.2), 518 (32.9), 517 (100), 455 (25.4) MS^3 [679 → 517]: 473 (20.1), 456 (100), 455 (80.1), 441 (21.9) MS^4 [679 → 517 → 456]: 392 (100)	Unknown	Leaves Flowers
40	27.7	–	593	MS^2 [593]: 447 (76.4), 285 (100) MS^3 [593 → 285]: 256 (71.0), 229 (100), 153 (75.5)	Kaempferol-*O*-coumaroyl hexoside	Leaves Flowers

"–" UV spectra have not been properly observed due to low intensity UV.

[a] Compared with a reference standard.

Table 2
Characterization of anthocyanins compounds of the water and ethanolic extracts from *Rubus grandifolius* Lowe by HPLC–DAD/ESI–MS^n in positive mode.

No.	t_R (min)	UV λ_{max} (nm)	$[M+H]^+$ *m/z*	HPLC-DAD-(+)ESI/MS^n *m/z* (% base peak)	Assigned identity	Sample
An1	2.7	522	449	MS^2 [449]: 288 (12.6), 287 (100) MS^3 [449 → 287]: 213 (21.9), 165 (40.2), 161 (100), 137 (59.6) MS^4 [449 → 287 161→]: 143 (100)	Cyanidin-*O*-hexoside	Water Ethanol
An2	5.4	300, 520	419	MS^2 [419]: 288 (14.3), 287 (100) MS^3 [419 → 287]: 259 (99.2), 231 (99.7), 221 (87.5), 137 (100), 115 (97.6)	Cyanidin-*O*-pentoside	Water Ethanol
An3	9.3	531	611	MS^2 [611]: 304 (15.6), 303 (100) MS^3 [611 → 303]: 257 (100), 229 (81.0) MS^4 [611 → 303 → 257]: 229 (100), 215 (12.9), 201 (20.3)	Delphinin-*O*-coumaroylhexoside0	Water Ethanol
An4	10.1	–	435	MS^2 [435]: 304 (21.9), 303 (100) MS^3 [435 → 303]: 274 (50.2), 257 (100), 229 (91.7), 201 (45.9), 165 (47.6) MS^4 [435 → 303 → 257]: 229 (100), 173 (41.4), 128 (32.4), 123 (28.1)	Delphinin-*O*-pentoside	Water Ethanol
An5	10.5	–	551	MS^2 [551]: 304 (16.7), 303 (100) MS3 [551 → 303]: 132 (33.5), 115 (15.8), 114 (100)	Delphinin-*O*-malonylhexoside	Water Ethanol
An6	13.6	526	449	MS^2 [449]: 318 (13.8), 317(100) MS^3 [449 → 317]: 302 (100), 285 (30.9), 261 (36.9) MS^4 [449 → 317 → 302]: 284 (45.8), 273 (16.6), 218 (100)	Petunidin-*O*-pentoside	Water

"–" UV spectra have not been properly observed due to low intensity.

fragments at *m/z*, characteristic of quercetin. As mentioned before, the favored substitution positions for flavonols, like quercetin, are positions 3-OH and 7-OH. Flavonols substituted at 3-OH position should present relative high intensity aglycone radical fragment, sometimes higher than the Y_0^- ion (Cuyckens and Claeys, 2005). Such pattern was not observed for this compound, thus, the glycosilation site could not be surely confirmed and compound **18** was tentatively identified as quercetin-*O*-glucuronide.

Another peak was detected at t_R = 10.1 min (compound **19**) exhibited a $[M-H]^-$ ion at *m/z* 433 and its fragmentation by MS^2 experiments showed a loss of 132 Da, probably due to a pentoside residue. MS^n fragmentation gave intense ions at *m/z* 271, 283, 257 and 229, which are similar with those obtained for a standard solution of ellagic acid and described in literature data (Simirgiotis et al., 2009). Ellagic acid is ahydroxybenzoic acids (polyphenols) that are commonly *O*-glycosylated. Hence, compound **19** was assigned as ellagic acid-*O*-pentoside.

Compound **20** (t_R = 10.8 min) gave a $[M-H]^-$ ion at *m/z* 477 and in the MS^2 fragmentation a neutral loss of 192 Da was observed to produce a fragment ion at *m/z* 285. This 192 Da residue was identified as hydroxyferulic acid.

The fragmentation of the ion at *m/z* 285 gave a fragment ion at *m/z* 255 (loss of 30 Da, $[Y_0^- – CH_2OH]^-$) which is characteristic of kaempferol (compared with a standard solution of kaempferol) (Olsen et al., 2009).

The linkage position of this group is not easy to establish based only on MS^n data, but an aglycone radical ion fragment was detected at *m/z* 284 with a relative peak intensity of 59.5%. Thus, compound **20** was identified as kaempferol-3-*O*-hydroxylferuloyl.

Compound **21** (t_R = 11.0 min) gave a $[M-H]^-$ ion at *m/z* 447 and in the MS^2 spectrum an ion at *m/z* 284, as base peak, and an intense ion at *m/z* 285 (70.3% of base peak). MS^3 fragmentation showed fragment ions characteristic to kaempferol (see compound **17**) and since the aglycone radical ion, at *m/z* 285, is the base peak this compound was characterized as kaempferol-3-*O*-hexoside.

Compound **22** (t_R = 11.7 min) displayed a $[M-H]^-$ ion at *m/z* 337 and showed a MS^n pattern typical of coumaroylquinic acids with main fragment ions at *m/z* 191 (MS^2) and *m/z* 147 (MS^3). The fragmentation pattern displayed by this compound is similar to 5-*O*-*p*-coumaroylquinic acid (Clifford et al., 2005); however, analysis of a solution of the standard compound showed a retention time of 8 min (data not presented). Thus, compound **22** was tentatively characterized as 1-*O*-*p*-coumaroylquinic acid.

Compound **23** (t_R = 11.8 min) gave a $[M-H]^-$ ion at *m/z* 503. In the MS^2 spectrum gave a fragment ion at *m/z* 179, as base peak (loss of 324 Da) and second peak at *m/z* 341 (loss of 162 Da) suggesting a combined loss of two residues of 162 Da that can be either a combination of two hexosides residues or one hexoside residue esterified with a caffeoyl. The last hypothesis was excluded given the absence of a fragment ion at *m/z* 323.

MS^n fragmentation of the ion at *m/z* 179 forming fragment ion at *m/z* 135 (loss of 44 Da) led to its identification as caffeic acid. Therefore, compound **23** was identified as caffeic acid-*O*-dihexoside. Lack of both standards and reported data made it impossible to assign the exact position of the hexose residue (Vallverdú-Queralt et al., 2011).

Compound **24** (t_R = 12.3 min) exhibited a $[M-H]^-$ at *m/z* 461 and eliminated a glucuronide residue in the MS^2 fragmentation. The MS^2 spectrum base peak is a fragment ion at *m/z* 285. MS^3 and MS^4 gave characteristic fragment ions of kaempferol. Substitution at position 3-OH is excluded because no deprotonated aglycone radical ion with high intensity was observed. So, compound **24** was identified as kaempfeol-*O*-glucuronide.

Compound **25** (t_R = 12.4 min) displayed a $[M-H]^-$ at *m/z* 417 and MS^2 fragmentation gave a neutral fragment of 132 Da (pentose) forming the aglycone ion (Y_0^-) at *m/z* 285. MS^n fragmentation resulted in the characteristic fragments of kaempferol (*m/z* 257, 255 and 229). The radical aglycone ion, *m/z* 284, was the base peak in the MS^2 spectrum indicating a 3-OH substituted flavonol. Consequently, compound **25** was characterized as kaempferol-3-*O*-pentoside.

Compound **26** (t_R = 12.5 min) was identified as 1,5-*O*-dicaffeoylquinic acid ($[M-H]^-$ at *m/z* 515) by comparison with a reference solution and our previous work (Gouveia and Castilho, 2009).

Compound **29** (t_R = 13.6 min) had a $[M-H]^-$ ion at *m/z* 547. In the MS^2 spectrum, a fragment ion at *m/z* 161 was observed (neutral loss of 386 Da). The ion at *m/z* 161 presented a fragment ion at *m/z* 133 (loss of 28 Da (CO)). This fragmentation is in agreement with those reported for umbelliferone, a coumarin (Wang and Feng, 2009).

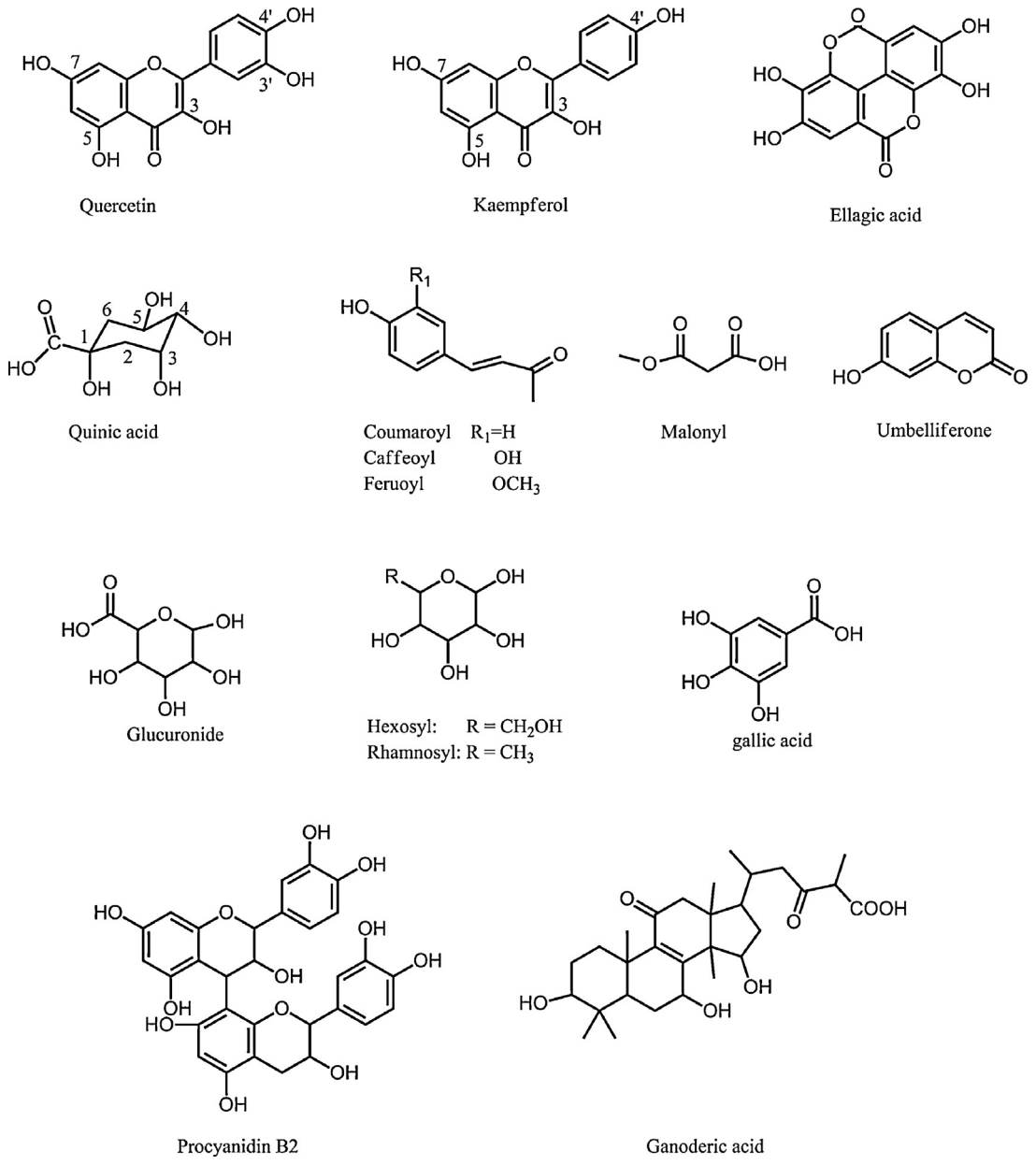

Fig. 1. Chemical structures of the main moieties identified in the phenolic profile of *Rubus grandifolius* Lowe.

Compounds **31** (t_R = 15.0 min), **33** (t_R = 18.3 min) and **37** (t_R = 24.8 min) exhibited the same deprotonated molecular ion $[M-H]^-$, at *m*/*z* 711.

In the MS^2 spectrum, a loss of 208 Da generating a fragment ion at *m*/*z* 503 was observed for all three compounds. This residue is probably an hexoside-acetyl residue (162 + 46 Da) as suggests the fragment ions at *m*/*z* 665 (−46 Da) and *m*/*z* 549 (−162 Da).

However, further MS^n fragmentation was distinct for all 3 compounds. For compound **31,** the fragment ion at *m*/*z* 503 gave a MS^3 base peak at *m*/*z* 485 (−18 Da, H_2O) and a MS^4 base peak at *m*/*z* 453

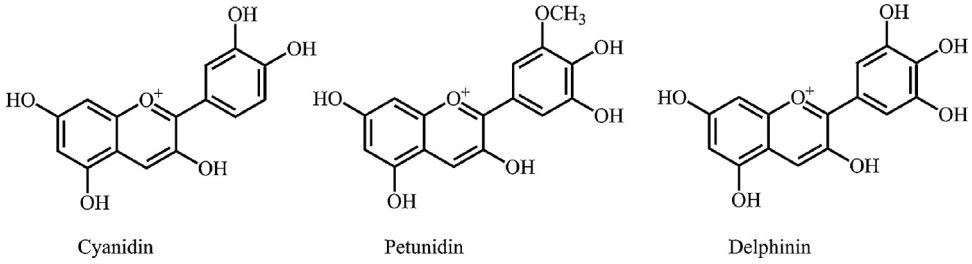

Fig. 2. Chemical structures of three anthocyanidins aglycones characterized in *Rubus grandifolius* Lowe.

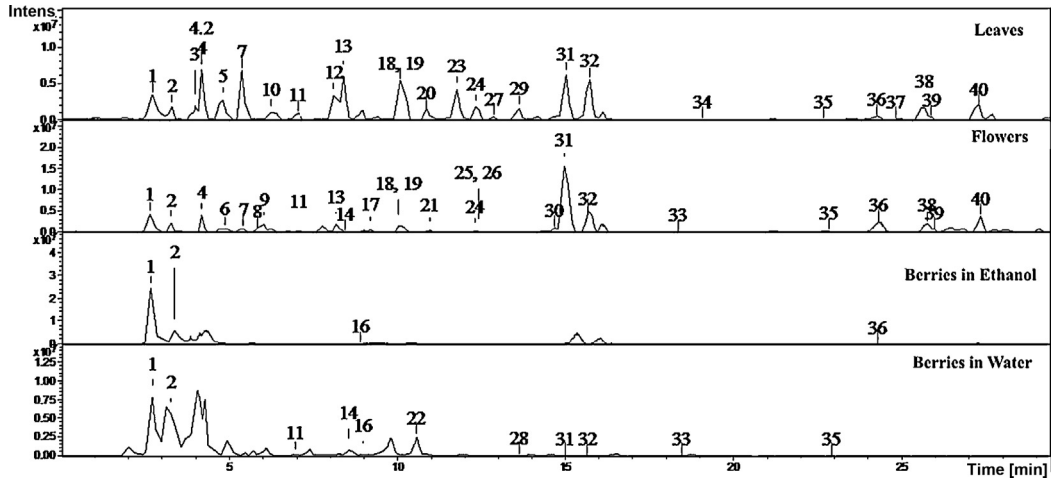

Fig. 3. HPLC–DAD-(−)ESI/MS^n base peak chromatogram chromatograms (BPC) of *Rubus grandifolius* Lowe leaves, flowers and berries (negative mode).

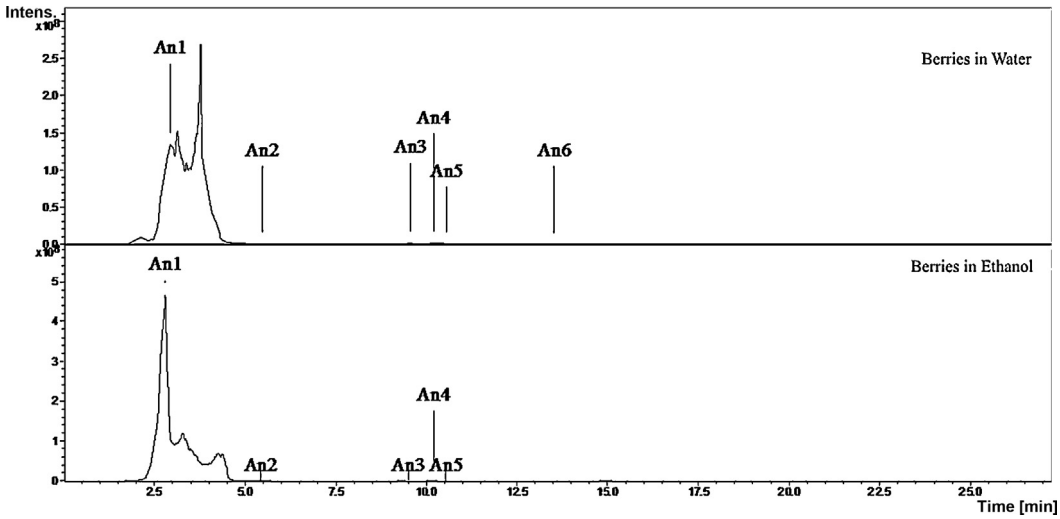

Fig. 4. HPLC–DAD-(+)ESI/MS^n chromatograms (base peak chromatogram – BPC) of *Rubus grandifolius* Lowe berries (positive mode).

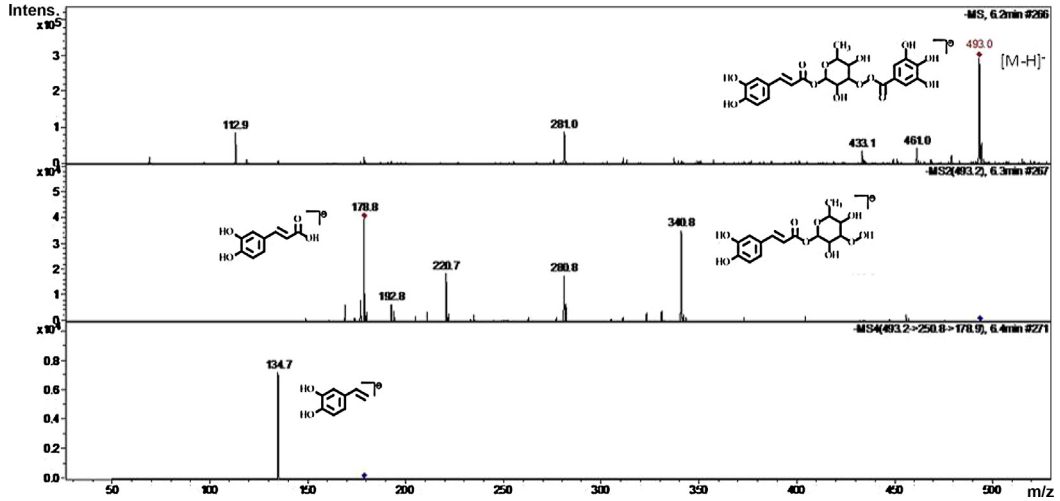

Fig. 5. ESI–MS^n negative mode of compound **10** – caffeic acid-*O*-galloylhexoside. Sequential fragmentation of the ion at *m*/*z* 493.

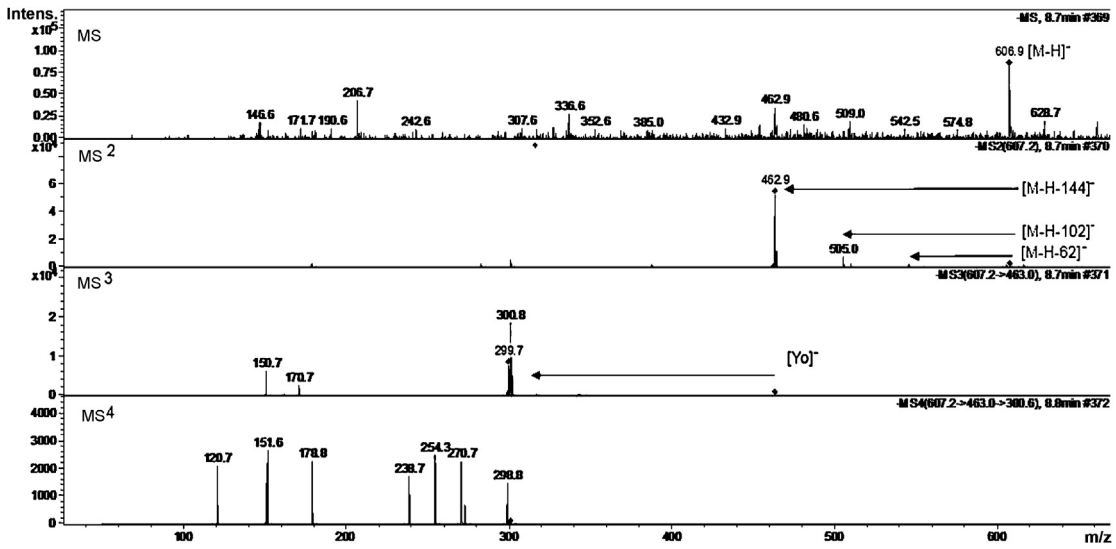

Fig. 6. ESI–MS^n negative mode of compound **15** – 3-hydroxy-3-methylglutaroyl of quercetin-7-*O*-hexoside. Sequential fragmentation, MS^n (n = 2–4) of the ion at m/z 607.

(−32 Da, CH_3OH) and an intense fragment ion at 409 (52.3% of base peak, −44 Da).

Compound **33** behaved different in the MS^4 fragmentation where the m/z 485 gave a fragment ion at m/z 421 (−44 Da, CO_2). Gao et al. (2011) described the fragmentation of compound **31** and **33,** and they were identified as diastereomers of triterpene acids. So, compounds **31** and **33** can be characterized as triterpene acid-*O*-hexoside acetyl.

Compound **37** was also characterized as a triterpene acid -*O*-hexoside acetyl, even if the MS^4 spectrum showed a distinct fragmentation (base peak at m/z 171).

Compounds **35** and **36** show a $[M-H]^-$ ion at m/z 709; in the MS^2, there is a loss of 208 similar to compounds **31**, **33** and **37**, probably given an hexoside-acetyl residue. Further fragmentation of the m/z ion of at 501, is not the same for this pair of compounds, so

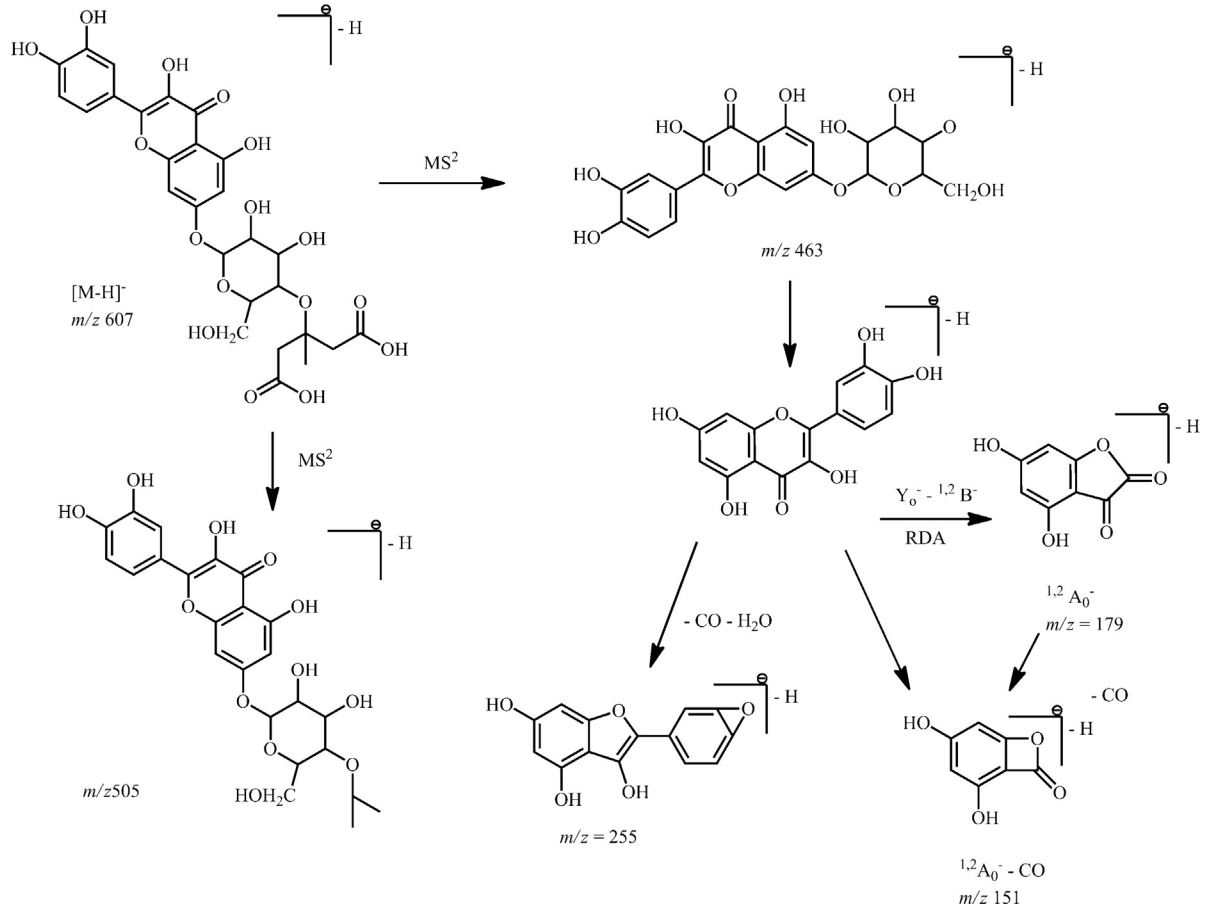

Fig. 7. Proposed fragmentation pathway for compound **15**.

they were characterized as triterpene acid acetyl hexosides without any further attempt to identify the structure of the terpene moiety.

Compound **32** (t_R = 15.7 min) gave a $[M-H]^-$ ion at *m/z* 679 and in the MS^2 spectrum displayed base peak at *m/z* 517 (loss of 162 Da, probably an hexoside residue). In the MS^2 spectrum, a molecule of water is expelled (−18 Da) forming a fragment ion at *m/z* 499. Fragmentation of this ion showed as main fragment ions at *m/z* 437 (base peak, −62 Da), *m/z* 455 (79.8%, −44 Da) and *m/z* 481 (24.9%, −18 Da). This pattern was described before as a triterpenic acic, more precisely ganoderic acid C2 (Yang et al., 2007). Thus, compound **32** was characterized as ganoderic acid C2 hexoside.

Compounds **38** (t_R = 25.6 min) and **40** (t_R = 27.7 min) exhibited the same $[M-H]^-$ at *m/z* 593. The MS^2 fragmentation lead to a base peak at *m/z* 285 due to the loss of 308 Da which was characterized as a combined loss of 162 + 146 Da proved by the $[M–H-146]^-$ ion at *m/z* 447. The high retention time of these compounds suggests that the neutral loss of 146 Da is due to a coumaroyl group rather than a rhamnose unit. The ion at *m/z* 285 corresponds to the deprotonated aglycone ion (Y_0) and its MS^n fragmentation gave the characteristic RDA fragments of kaempferol.

The linkage position of the coumaroyl group is difficult to establish based only on the MS^n data, thus, compound **38** and compound **40** were characterized as kaempferol-*O*-coumaroyl hexosides. Tiliroside is a kaempferol-*O*-coumaroyl hexoside frequently found in *Rubus* (Lu et al., 2009), but without a standard sample, it was not possible to establish the effective identity.

Compound **16** (t_R = 8.9 min) showed a $[M-H]^-$ ion at *m/z* 523. In the MS^n fragmentation the main fragment ions were MS^2 *m/z* 475 (loss of 48 Da), MS^3 *m/z* 329 (loss of 146 Da) and MS^4 *m/z* 314 (loss of 15 Da, probably a methoxy group). Based only on these data and UV DAD analysis, it was not possible to characterize this compound.

Compound **30** (t_R = 14.3 min) exhibited a $[M-H]^-$ ion at *m/z* 695. The MS^2 spectrum revealed a fragment ion at *m/z* 485 (loss of 210 Da). The MS^3 fragmentation indicates the loss of a water molecule (−18 Da) with a fragment ion at *m/z* 467 and followed with the loss of CO_2 group (−44 Da) in the MS^4 fragmentation (*m/z* 423). With only these MS^n data it was not possible to identify the nature of compound **30**.

Compound **34** (t_R = 19.0 min) gave a $[M-H]^-$ ion at *m/z* 479 and the MS^n experiments conducted to three consecutive losses of 94 Da.

3.1.2. Positive mode ionization

The pigments in berries are mainly anthocyanins, which are more easily characterized with positive mode (ESI^+) electrospray ionization combined with UV–DAD characteristic absorptions (520 nm). The MS and UV data used to identify anthocyanins in *R. grandifolius* Lowe berries extracts are summarized in Table 2.

In the ESI^+ experiments, the protonated molecular ion ($[M+H]^+$) and the fragment ions $[M+H–X]^+$ are observed and, since anthocyanins present a natural residual positively charged, it is possible to detect also a true molecular ion $[M]^+$ and a fragment ion $[M–X]^+$. The fragment ion is that of the underivatized aglycone (Abdel-Aal et al., 2006).

The ESI^+ analysis of the several extracts was only relevant for the berries samples. Some of the flavonoids conjugates detected with ESI^- were also found in the ESI^+ however with a much lower peak resolution associated to the known lowest sensitivity of this type of ionization for these compounds.

Five anthocyanins aglycones were characterized as different glycosylates.

The most common positions for glycosylation in anthocyanins are positions 3-OH and 5-OH. However, in this work the MS^n data obtained did not provide enough information in order to establish the exact glycosylation position.

Compound **An1** (t_R = 2.7 min) gave a $[M+H]^+$ ion at *m/z* 449 and in the MS^2 fragmentation a fragment ion at *m/z* 287 was observed due to neutral loss of a 162 Da moiety (probably an hexose residue). The hypothesis of this compound being a kaempferol derivative was excluded given the UV–DAD data and since in the negative mode, at the same retention time, no kaempferol derivative was detected. Further fragmentation of the ion at *m/z* 287 suggests that the aglycone is cyanidin based on literature data (Felgines et al., 2005). Thus, compound **An1** was characterized as cyanidin-*O*-hexoside.

Compound **An2** (t_R = 5.4 min) exhibited a $[M+H]^+$ ion at *m/z* 419. The MS^2 fragmentation reveals a neutral cleavage of 132 Da leading to the fragment ion at *m/z* 287. Subsequent fragmentation of this ion gave typical fragments of cyanidin. The 132 Da neutral loss can be attributed to a pentose (arabinose, xylose or apiose) or to a tartaric acid unit. Considering the low retention time of this compound, the hypothesis of a tartaric acid unit was excluded. Therefore, compound **An2** was characterized as cyanidin-*O*-pentoside.

Compound **An3** (t_R = 9.3 min) exhibited a $[M+H]^+$ ion at *m/z* 611 and easily lost a 308 Da residue forming a fragment ion at *m/z* 303. MS^n fragmentation of this ion revealed fragment ions at *m/z* 257, 229 and 173 consistent to those reported for delphinine (Downey and Rochfort, 2008). The 308 Da moiety can possibly be composed of a caffeoyl group (162 Da) and a coumaroyl group (146 Da). Since the fragment ion correspondent to the individual loss of a coumaric acid and hexose units was not observed the two groups should be linked in the same position of the aglycone. So, compound **An3** was characterized as delphinin-*O*-coumaroylhexoside.

Compound **An4** (t_R = 10.1 min) was characterized as delphinin-*O*-pentoside. This compound showed a $[M+H]^+$ ion at *m/z* 435 and the MS^n experiments resulted in a neutral loss of 132 Da (MS^2) and typical fragments of delphinin (MS^3 and MS^4).

Delphinin was also found to be the aglycone for compound **An5** (t_R = 10.5 min) with a $[M+H]^+$ of *m/z* 551. The MS^2 fragment ion of 248 Da was characterized as malonylhexoside residue and compound **An5** will be a delphinin-*O*-malonylhexoside.

Compound **An6** (t_R = 13.6 min) exhibited a $[M+H]^+$ ion at *m/z* 449 and in the MS^2 spectrum a neutral loss of 132 Da (pentoside). MS^n fragmentation allowed for the characterization of the fragment ion at *m/z* 317 as petunidin with typical fragments at *m/z* 302, 261, 285 and 218 (Downey and Rochfort, 2008). So, **An6** should be a petunidin pentoside.

3. 2 Antioxidant capacity

The phenolic composition of plant extracts and berries is associated to its antioxidant properties and different antioxidant mechanisms are present in these complex samples.

The assessment of antioxidant capacity of each sample was performed by three distinct assays: DPPH and ABTS radical scavenging activity and FRAP assay (ET method).

Employing several methods to measure antioxidant activity can give the impressions of redundancy but since different authors used distance methods, comparison of properties becomes easier if a large set of data is gathered (Gouveia-Figueira et al., 2014).

The values obtained for the antioxidant activity are shown in Table 3.

DPPH method gave values in a wide range, varying from 10.1 ± 0.1 μmol eq Trolox/100 g Trolox/100 g (flowers in methanol) to 147.9 ± 0.7 μmol eq Trolox/100 g (berries in ethanol).

For ABTS assay, the flowers also presented the lowest antioxidant capacity (22.4 ± 0.5 μmol eq Trolox/100 g) and the ethanolic extracts of the berries the highest capacity (255.8 ± 1.9 μmol eq Trolox/100 g^{-1}).

The ABTS assay values were higher than the DPPH assay, and as it was described before in our group for other sets of plants (Gouveia

Table 3
Rubus grandifolius Lowe experimental determinations of antioxidant capacity against DPPH, ABTS and FRAP.

Rubus grandifolius Lowe	Leaves	Flowers	Berries	
			Water	Ethanol
DPPH (μmol eq Trolox/g DM)	98.4 ± 1.9	10.1 ± 0.1	121.1 ± 1.5	147.9 ± 0.7
ABTS (μmol eq Trolox/g DM)	113.0 ± 1.2	22.4 ± 0.5	214.9 ± 1.8	255.8 ± 1.9
FRAP (mmol Fe(II)/mg DM)	5122 ± 34	3241 ± 41	ND	9455 ± 29

DM – Dried material, with exception for the berries where fresh weight was used; ND – not determined.

and Castilho, 2011a, 2012c) is mainly related to the different sensitivity of both methods.

The FRAP assay establishes the antioxidant capacity based on the sample reducing ability. Once more, the ethanolic extract of the berries showed higher antioxidant capacity with a FRAP value of 9455 ± 29 mmol Fe(II)/mg.

The comparison of antioxidant capacity values between different laboratories is always tricky and should be attempted carefully, because it is difficult to use the exactly same experimental conditions.

Deighton et al. (2000) reported the antioxidant of several *Rubus* berries. Comparing those results with ours, it is possible to conclude that endemic Madeira *R. grandifolius* Lowe berries have a higher radical scavenging activity (ABTS assay), 10 times higher than Deighton's most active species; however, their reducing power is mild: Deighton found a wide disparity of activity in the FRAP assay, ranging from about 190–65,700 μmol ferrous ion, the value for *R. grandifolius* being about 9500. Climate may be the key issue here. The reducing capacity (FRAP assay) of red raspberries cultivated at different conditions was found to increase with harvesting temperature (~30 °C) and also with high levels of cyanidin-*O*-glucosides and quercetin-*O*-glucosides (Bradish et al., 2011). The mild reducing properties of *R. grandifolius* Lowe can be associated to the location where the plant material was collected at Santo da Serra (average temperature 25 °C during the harvesting season and high humidity levels) that may not promote the biosynthesis of the most active compounds. More important, it is known that light stimulates the synthesis of flavonoids, especially anthocyanins and flavones, phenylalanine ammonialyase being the major inducible enzyme these UV-absorbing compounds are thought to provide a means of protection against UV-B damage. (Alothman et al., 2009; Winkel-Shirley, 2002) It is thought that phenolic compounds help to attenuate the amount of light reaching the photosynthetic cells, since these UV-absorbing compounds are thought to provide a means of protection against UV-B damage. In Madeira, *R. grandifolius* grows mainly on the shady paths of the dense Laurissilva endemic forest, never being exposed to direct sunlight for long hours.

The berries presented a highest antioxidant capacity when compared with other morphological parts, this being probably associated to the presence of anthocyanins in the berries as main components.

There are not many scientific studies on the assessment of antioxidant capacity of *Rubus* aerial parts to compare our results with. Nevertheless, the same antioxidant assays described in this paper were applied to other plant extracts (Gouveia-Figueira et al., 2014; Gouveia and Castilho, 2011b, 2012b) and it possible to infer that *R. grandifolius* Lowe leaves present a high antioxidant capacity, while the flowers extracts presented a weak antioxidant capacity.

Through the qualitative phenolic profile characterization by HPLC–DAD–ESI/MS^n such a different behavior between the leaves and the flowers was not observed, thus, the distinct antioxidant capacity must be related to the amounts of the compounds present in the leaves and flowers and/or other classes of compounds rather than phenolic compounds.

4. Conclusion

About forty phenolic compounds were detected in polar extracts of wild *R. grandifolius* Lowe (leaves, flowers and berries) such as flavonoids, anthocyanins, glycosylated triterpenes and conjugated forms of hydroxycinnamic acids. Twenty five compounds were found in leaves and flowers and seventeen in berries, these comprising six anthocyanins; two procyanidins were found in leaves. Six triterpene glycosides were ubiquitous in the various morphological parts.

As opposed to other *Rubus* species, ellagintannins were not detected; only one ellagic acid derivative was identified.

Among the flavonoids, quercetin and kaempferol conjugates (flavonol type) were the main components. In the negative ionization mode, the phenolic profile of the berries extracts was quite different, since the water extract only showed three compounds (also present in the ethanolic extract). In positive mode, similar anthocyanins profiles were found.

In addition, the antioxidant capacity was also measured and good radical scavenger activity (DPPH and ABTS assays) and mild reducing properties (FRAP assay) were found. The flowers are the morphological part with lowest antioxidant capacity while the ethanolic extracts of the berries are the most active part of *R. grandifolius* Lowe. Despite that the phenolic composition of the water extract was much less diversified than the ethanolic extract, the antioxidant capacity is in the same order.

Further studies are currently under consideration to understand better how the phenolic composition is related to the folk medicine applications of this plant.

Acknowledgements

S. Gouveia-Figueira is grateful to Fundação para a Ciência e Tecnologia (FCT) for a Ph.D. grant SFRH/BD/24227/2005. The mass spectrometer used in this work is part of the Portuguese National Mass Spectrometry Network (Contract RNEM-REDE/1508/REM/2005) and was purchased in the framework of the National Programme for Scientific Re-equipment, with funds from POCI 2010 (FEDER) and FCT. Mrs. Conceição Pires is recognized for excellent assistance in sample collection.

References

Abdel-Aal, E.-S.M., Young, J.C., Rabalski, I., 2006. Anthocyanin composition in black, blue, pink, purple, and red cereal grains. J. Agric. Food Chem. 54, 4696–4704.
Ablajan, K., Abliz, Z., Shang, X.-Y., He, J.-M., Zhang, R.-P., Shi, J.-G., 2006. Structural characterization of flavonol 3,7-di-*O*-glycosides and determination of theglycosylation position by using negative ion electrospray ionization tandem mass spectrometry. J. Mass Spectrom. 41, 352–360.
Alothman, M., Bhat, R., Karim, A.A., 2009. Effects of radiation processing on phytochemicals and antioxidants in plant produce. Trends Food Sci. Technol. 20, 201–212.
Bobinaitė, R., Viškelis, P., Venskutonis, P.R., 2012. Variation of total phenolics anthocyanins, ellagic acid and radical scavenging capacity in various raspberry (*Rubus* spp.) cultivars. Food Chem. 132, 1495–1501.
Bradish, C.M., Perkins-Veazie, P., Fernandez, G.E., Xie, G., Jia, W., 2011. Comparison of flavonoid composition of red raspberries (*Rubus idaeus* L.) Grown in the Southern United States. J. Agric. Food Chem. 60, 5779–5786.
Clifford, M.N., Knight, S., Kuhnert, N., 2005. Discriminating between the six isomers of dicaffeoylquinic acid by LC–MS^n. J. Agric. Food Chem. 53, 3821–3832.

Cuyckens, F., Claeys, M., 2004. Mass spectrometry in the structural analysis of flavonoids. J. Mass Spectrom. 39, 1–15.
Cuyckens, F., Claeys, M., 2005. Determination of the glycosylation site in flavonoid mono-*O*-glycosides by collision-induced dissociation of electrospray-generated deprotonated and sodiated molecules. J. Mass Spectrom. 40, 364–372.
Deighton, N., Brennan, R., Finn, C., Davies, H.V., 2000. Antioxidant properties of domesticated and wild *Rubus* species. J. Sci. Food Agric. 80, 1307–1313.
Downey, M.O., Rochfort, S., 2008. Simultaneous separation by reversed-phase high-performance liquid chromatography and mass spectral identification of anthocyanins and flavonols in Shiraz grape skin. J. Chromatogr. A 1201, 43–47.
Felgines, C., Talavera, S., Texier, O., Gil-Izquierdo, A., Lamaison, J.-L., Remesy, C., 2005. Blackberry anthocyanins are mainly recovered from urine as methylated and glucuronidated conjugates in humans. J. Agric. Food Chem. 53, 7721–7727.
Gao, J., Shi, J., Lu, X., Sun, C., Pan, Y., 2011. Differentiation of common diastereoisomeric ursane-type triterpenoids by high-performance liquid chromatography/tandem mass spectrometry. Rapid Commun. Mass Spectrom. 25, 1349–1355.
Gouveia-Figueira, S., Gouveia, C., Carvalho, M., Rodrigues, A., Nording, M., Castilho, P., 2014. Antioxidant capacity, cytotoxicity and antimycobacterial activity of madeira archipelago endemic *Helichrysum* dietary and medicinal plants. Antioxidants 3, 713–729.
Gouveia, S.C., Castilho, P.C., 2009. Analysis of phenolic compounds from different morphological parts of *Helichrysum devium* by liquid chromatography with on-line UV and electrospray ionization mass spectrometric detection. Rapid Commun. Mass Spectrom. 23, 3939–3953.
Gouveia, S.C., Castilho, P.C., 2010. Characterization of phenolic compounds in *Helichrysum melaleucum* by high-performance liquid chromatography with on-line ultraviolet and mass spectrometry detection. Rapid Commun. Mass Spectrom. 24, 1851–1868.
Gouveia, S.C., Castilho, P.C., 2011a. Antioxidant potential of *Artemisia argentea* L'Hér alcoholic extract and its relation with the phenolic composition. Food Res. Int. 44, 1620–1631.
Gouveia, S.C., Castilho, P.C., 2011b. Characterisation of phenolic acid derivatives and flavonoids from different morphological parts of *Helichrysum obconicum* by a RP-HPLC–DAD-(−)-ESI–MS^n method. Food Chem. 129, 333–344.
Gouveia, S., Castilho, P.C., 2012a. *Helichrysum monizii* Lowe: phenolic composition and antioxidant potential. Phytochem. Anal. 23, 72–83.
Gouveia, S.C., Castilho, P.C., 2012b. *Helichrysum monizii* Lowe: phenolic composition and antioxidant potential. Phytochem. Anal. 23, 72–83.
Gouveia, S.C., Castilho, P.C., 2012c. Phenolic composition and antioxidant capacity of cultivated artichoke, Madeira cardoon and artichoke-based dietary supplements. Food Res. Int. 48, 712–724.
Hummer, K.E., 2010. Rubus pharmacology: antiquity to the present. HortScience 45, 1587–1591.
Jaakkola, M., Korpelainen, V., Hoppula, K., Virtanen, V., 2012. Chemical composition of ripe fruits of *Rubus chamaemorus* L. grown in different habitats. J. Sci. Food Agric. 92, 1324–1330.
Kajdžanoska, M., Gjamovski, V., Stefova, M., 2010. HPLC–DAD–ESI–MS^n identification of phenolic compounds in cultivated strawberries from Macedonia. Maced. J. Chem. Chem. Eng. 29, 181–194.
Kusznierewicz, B., Piekarska, A., Mrugalska, B., Konieczka, P., Namieśnik, J., Bartoszek, A., 2012. Phenolic composition and antioxidant properties of polish blue-berried honeysuckle genotypes by HPLC–DAD–MS, HPLC postcolumn derivatization with ABTS or FC, and TLC with DPPH visualization. J. Agric. Food Chem. 60, 1755–1763.
Chen, Y.-H., Wang, Z.-T., Tao, X.-Y., 2009. Tyrosinase inhibitory effect and inhibitory mechanism of tiliroside from raspberry. J. Enzyme Inhib. Med. Chem. 24, 1154–1160.
Mabry, T.J., Markham, K.R., Thomas, M.B., 1970. The ultraviolet spectra of flavones and flavonols, isoflavones, dihydroxyflavonols. In: Springer-Verlag (Ed.), The Systematics Identification of Flavonoids. Springer-Verlag, New York, NY.
Olsen, H., Aaby, K., Borge, G.I.A., 2009. Characterization and quantification of flavonoids and hydroxycinnamic acids in curly kale (*Brassica oleracea* L. Convar. *acephala* Var. *sabellica*) by HPLC–DAD–ESI–MS^n. J. Agric. Food Chem. 57, 2816–2825.
Pereira, O.R., Silva, A.M.S., Domingues, M.R.M., Cardoso, S.M., 2012. Identification of phenolic constituents of *Cytisus multiflorus*. Food Chem. 131, 652–659.
Re, R., Pellegrini, N., Proteggente, A., Pannala, A., Yang, M., Rice-Evans, C., 1999. Antioxidant activity applying an improved ABTS radical cation decolorization assay. Free Radical Bio. Med. 26, 1231–1237.
Rivera, D., Obón, C., 1995. The ethnopharmacology of Madeira and Porto Santo Islands, a review. J. Ethnopharm. 46, 73–93.
Scordino, M., Sabatino, L., 2014. Characterization of polyphenolic profile of citrus fruit by HPLC/PDA/ESI/MS–MS. In: Watson, R.R. (Ed.), Polyphenols in Plants. Academic Press, San Diego, pp. 187–199 (Chapter 9).
Sejali, S.N.F., Anuar, M.S., 2011. Effect of drying methods on phenolic contents of neem (*Azadirachta indica*) leaf powder. J. Herbs Spices Med. Plants 17, 119–131.
Simirgiotis, M.J., Theoduloz, C., Caligari, P.D.S., Schmeda-Hirschmann, G., 2009. Comparison of phenolic composition and antioxidant properties of two native Chilean and one domestic strawberry genotypes. Food Chem. 113, 377–385.
Soong, Y.Y., Barlow, P.J., 2005. Isolation and structure elucidation of phenolic compounds from longan (*Dimocarpus longan* Lour.) seed by high-performance liquid chromatography–electrospray ionization mass spectrometry. J. Chromatogr. A 1085, 270–277.
Tang, J., Zhao, M., Wang, Y., Kang, G., Wu, J., Zheng, M., Peng, S., 2011. One single HPLC–PDA/(−)ESI–MS/MS analysis to simultaneously determine 30 components of the aqueous extract of *Rabdosia rubescens*. J. Chromatogr. B 879, 2783–2793.
Turland, N.J., 1994. Flora da Madeira, HMSO Publications Center, first ed., London.
Vallverdú-Queralt, A., Jáuregui, O., Di Lecce, G., Andrés-Lacueva, C., Lamuela-Raventós, R.M., 2011. Screening of the polyphenol content of tomato-based products through accurate-mass spectrometry (HPLC–ESI–QTOF). Food Chem. 129, 877–883.
Wang, H., Feng, F., 2009. Identification of components in Zhi-Zi-Da-Huang decoction by HPLC coupled with electrospray ionization tandem mass spectrometry, photodiode array and fluorescence detectors. J. Pharm. Biomed. Anal. 49, 1157–1165.
Winkel-Shirley, B., 2002. Biosynthesis of flavonoids and effects of stress. Curr. Opin. Plant Biol. 5, 218–223.
Yang, M., Wang, X., Guan, S., Xia, J., Sun, J., Guo, H., Guo, D.-A., 2007. Analysis of triterpenoids in *Ganoderma lucidum* using liquid chromatography coupled with electrospray ionization mass spectrometry. J. Am. Soc. Mass Spectrom. 18, 927–939.